Journal of Ceramic Processing Research. Vol. 22, No. 1, pp. 31~38 (2021)
(Received 18 May 2020, Received in revised form 15 July 2020, Accepted 6 October 2020)
https://doi.org/10.36410/jcpr.2021.22.1.31

J O U R N A L O F
Ceramic Processing Research

Oxidation behavior of C/C composites with B_4C-SiC-ZrC-ZrB_2 coating prepared by infiltration and pyrolysis

Xiao-Hua Zuo[a,b,*], Zhi-Jun Dong[c], Guan-Ming Yuan[c], Zheng-Wei Cui[c] and Xuan-Ke Li[c]
[a]*School of Chemistry & Chemical Engineering, Hubei Polytechnic University, Huangshi 435003, China*
[b]*Hubei Key Laboratory of Mine Environmental Pollution Control & Remediation, Huangshi 435003, China*
[c]*Hubei Province Key Laboratory of Coal Conversion & New Carbon Materials, Wuhan University of Science and Technology, Wuhan 430081, China*

Polycarbosilane, B-Si and B-Si-Zr modification coal tar pitch were used as impregnate agent for infiltration and pyrolysis formation of carbon/carbon (abbreviated as C/C) composites with B_4C-SiC-ZrC-ZrB_2 coating. The density of the composites was examined to be 1.0 g·cm^{-3}, 1.4 g·cm^{-3} and 1.8 g·cm^{-3}, respectively. The phase compositions, surface morphologies and element distributions of the coating were analyzed by X-ray diffraction (XRD) scanning electron microscopy (SEM) and energy dispervive spectroscopy (EDS), respectively. The result showed that the two composites with a density of 1.4 g·cm^{-3} and 1.8 g·cm^{-3} displayed compact microstructures. The oxidation behavior of the composites was studied by oxidation in air at temperatures from 800 to 1,550 °C for 1 h. The composites with a density of 1.8 g·cm^{-3} exhibited a lower weight loss of 1.8 % after oxidation. B_4C-SiC-ZrC-ZrB_2 coating was found to provide the best protection by the precipitated B_2O_3, SiO_2 and ZrO_2 on the surface of the composites during the oxidation process, which were characterized by self-healing and anti-oxidation. The C/C composites with B_4C-SiC-ZrC-ZrB_2 coating performed well at high temperatures with the formation of complex oxides glass film that prevented oxygen from further spreading into the matrix.

Keywords: B_4C-SiC-ZrC-ZrB_2 coating, C/C composites, Oxidation resistance, Self-healing.

Introduction

Carbon/carbon (abbreviated as C/C) composites have attracted much attention for high temperature structural applications due to their excellent properties of lightweight, strength, thermal stability and ablation resistance [1, 2]. However, C/C composites are easily oxidized at a temperature above 400 °C, which limits their their extensive application in air [3, 4]. Therefore, oxidation barrier protection has been proposed to solve the problem and extend the service life of carbon materials. In recent research, ceramics coating was found to effectively improve oxidation resistance of C/C composites [5]. Introducing B_4C-SiC was reported to enhance greatly the oxidation resistance of C/C composites in atmosphere at high temperatures. The SiO_2 and B_2O_3 derived from the coating will seep into the composites and form a coating layer when B_4C-SiC were oxidized. The corresponding borosilicate film can prevent the gasification of boron oxide over 1,000 °C [6, 7]. The SiO_2 and B_2O_3 films were characterized by self-healing, anti-oxidation synergism and excellent oxidation resistance [5]. However, SiO_2 and B_2O_3 were detected to decompose and volatilize rapidly when the ambient temperature reached 1,500 °C. In addition, the physical and mechanical properties of C/C composites will deteriorate seriously when the glass protective layer is destroyed [8]. Therefore, more effort should be taken in order to elevate the oxidation resistance and prolong service life of C/C composites. Ultra-high temperature ceramics ZrC and ZrB_2 are put forward to satisfy these needs owing to their high melting point and mechanical properties [9]. The excellent physical and chemical compatibility for the above ceramics have attracted increasing attention in recent years [10]. ZrB_2 coating on C/C composites was reported to be prepared by dipping ZrB_2 in phenolic resin slurry, which was oxidized into ZrO_2 and B_2O_3 when exposed to air atmosphere above 1,400 °C, forming a continuous protective film [11, 12]. Studies have shown that surface microstructure modification of C/C-ZrC-SiC composites is an effective way to improve the stability of SiO_2 [13]. ZrB_2-SiC ceramics were observed to exhibit outstanding high temperature stability as well as good thermal oxidation resistance [14]. A ZrB_2-SiC/SiC gradient coating was successfully synthesized through adjusting the reaction temperature. Compared with the simple SiC coating, the gradient coating revealed a better ablation resistance, which could prevent C/C composite from ablation under the temperature of 2,500 °C and lasting time of 300 s [15]. Boron addition was found to have a

*Corresponding author:
Tel : +86 0714 6348825
Fax: +86 0714 6348814
E-mail: zuoxiaohua111@163.com

significant influence on the thermal cycling resistance and long-term oxidation resistance of ZrB_2-SiC coating [16]. At the same time, Zr-Si-B-C system was promoted to achieve better oxidation resistance in wide temperature domain in practical applications. This is due to the oxidation products of Zr-Si-B-C multiphase ceramic in the ablation process could be used as compensation oxide melts for the healing of cracks and holes on the matrix surface in different temperature ranges and effectively prevent the external heat from spreading into the matrix [17].

B_4C-SiC-ZrC-ZrB_2 coating for C/C composites has been prepared in this work for the sake of protecting C/C substrate by means of infiltration and pyrolysis, which is synthesized to the B-Si and B-Si-Zr modified coal tar pitch in the experiment. Because the B-Si and B-Si-Zr modified coal tar pitch can dissolve in toluene solution. B_4C-SiC-ZrC-ZrB_2 coating for C/C composites can easily be controlled during impregnation process with B-Si and B-Si-Zr modification coal tar pitch as impregnate agent. The microstructures, component and oxidation resistant of C/C composites have been investigated. The purpose is to examine the contribution of oxide formation to the microstructure and oxidation resistant of the composites.

Experiments

Synthesis of B-Si and B-Si-Zr modified coal tar pitch

All raw materials in this research are commercially available, including coal tar pitch, pyridine borane, polycarbosilane and zirconium diboride precursor (Sinopharm Chemical Reagent Co., Ltd.). Coal tar pitch was grinded and extracted in toluene solution. The soluble components were removed from the toluene solution by distillation. Then the toluene soluble fraction of coal tar pitch was obtained by drying. The softening point and pyrolysis yield of the toluene soluble fraction were examined to 52.4 ºC and 39.5 wt.%, respectively.

The prepared toluene soluble fractions, polycarbosilane, pyridine borane and zirconium diboride precursor were mixed to dissolve in toluene solution. And then, the mixture took place reaction at 180 ºC for 6 h in flask with condenser pipe. After that, the toluene solution was removed by distillation method. The resultant residue (a soluble brown solid) in flask was B-Si or B-Si-Zr modified coal tar pitch that could dissolved by toluene solution.

Preparation of B_4C-SiC-ZrC-ZrB_2 coating for C/C composites

Carbon fiber braid was impregnated by mesophase pitch through different cycle times in autoclave. The C/C composites were prepared and examined to have the density of 1.0 $g\cdot cm^{-3}$, 1.4 $g\cdot cm^{-3}$ and 1.8 $g\cdot cm^{-3}$, respectively. With polycarbosilane, B-Si and B-Si-Zr modification coal tar pitch as impregnate agent, three kinds of C/C composites were prepared by immersing under vacuum condition and cyclic heat treatment under the condition of 1,600 ºC and 6 h in argon atmosphere. The cyclic heat treatment was prepared for the sake of continuous infiltration and pyrolysis of the materials. Finally, The C/C composites with B_4C-SiC-ZrC-ZrB_2 coating were exposed to another heat treatment at 800-1,550 ºC in air for 1 h. The samples for D1.0, D1.4 and D1.8 hereafter refer to the composite sample with the density of 1.0, 1.4 and 1.8 $g\cdot cm^{-3}$, respectively.

Characterization

Phase compositions for C/C composites with B_4C-SiC-ZrC-ZrB_2 coating were examined by a Philips X'pert PBO X-ray diffractometer using Cu $K\alpha$ radiation. The densities of the composite specimens were measured by Archimedes method with ethyl alcohol as the medium. A scanning electron microscope (TESCAN VEGA3, provided by Chech) was used to observe the morphology of the C/C composites before and after oxidation. SEM is equipped with BRUKER 410-M energy chromatograph (EDS), which makes semi-quantitative composition analysis of sample. C/C composites were embedded in the resin. The composites were treated by MoPao 1,000-type metallurgical polishing machine. The microstructure of the C/C composites was observed by polarizing electronic microscope.

Results and Discussions

Fig. 1 shows the microstructures of the C/C composites observed by SEM and polarizing electronic microscope. The C/C composites with the density of 1.0 $g\cdot cm^{-3}$ revealed loose structure. There exist some pores between fiber bundles, providing a channel for impregnation of precursors (Fig. 1(a) and Fig. 1(b)). C/C composites with the density of 1.4 $g\cdot cm^{-3}$ showed small pores with the diameter of around 100 μm (Fig. 1(c) and Fig. 1(d)). The specimen with the density of 1.8 $g\cdot cm^{-3}$ displayed a compact structure, which was filled with pitch carbon (Fig. 1(e) and Fig. 1(f)). The porosity of C/C composites with the density of 1.0 $g\cdot cm^{-3}$, 1.4 $g\cdot cm^{-3}$ and 1.8 $g\cdot cm^{-3}$ was examined to be 38.1%, 20.7% and 2.6%, respectively. This indicates that the density of C/C composites is higher, the porosity is smaller. The pitch carbon filled in fiber bundles was assumed to be anisotropic (Fig. 1(b), 1(d), 1(f)).

Fig. 2 shows SEM images of C/C composites with B_4C-SiC-ZrC-ZrB_2 coating after heat treatment at 1,200 ºC. The surface of the composites with density of 1.0 $g\cdot cm^{-3}$ revealed a large number of micro-cracks and some holes with the diameter of about 40 μm in local area due to the peeling of the surface coating (Fig. 2(a)). For the sample with the density of 1.4 $g\cdot cm^{-3}$, a large number of cracks with width of ca. 10-

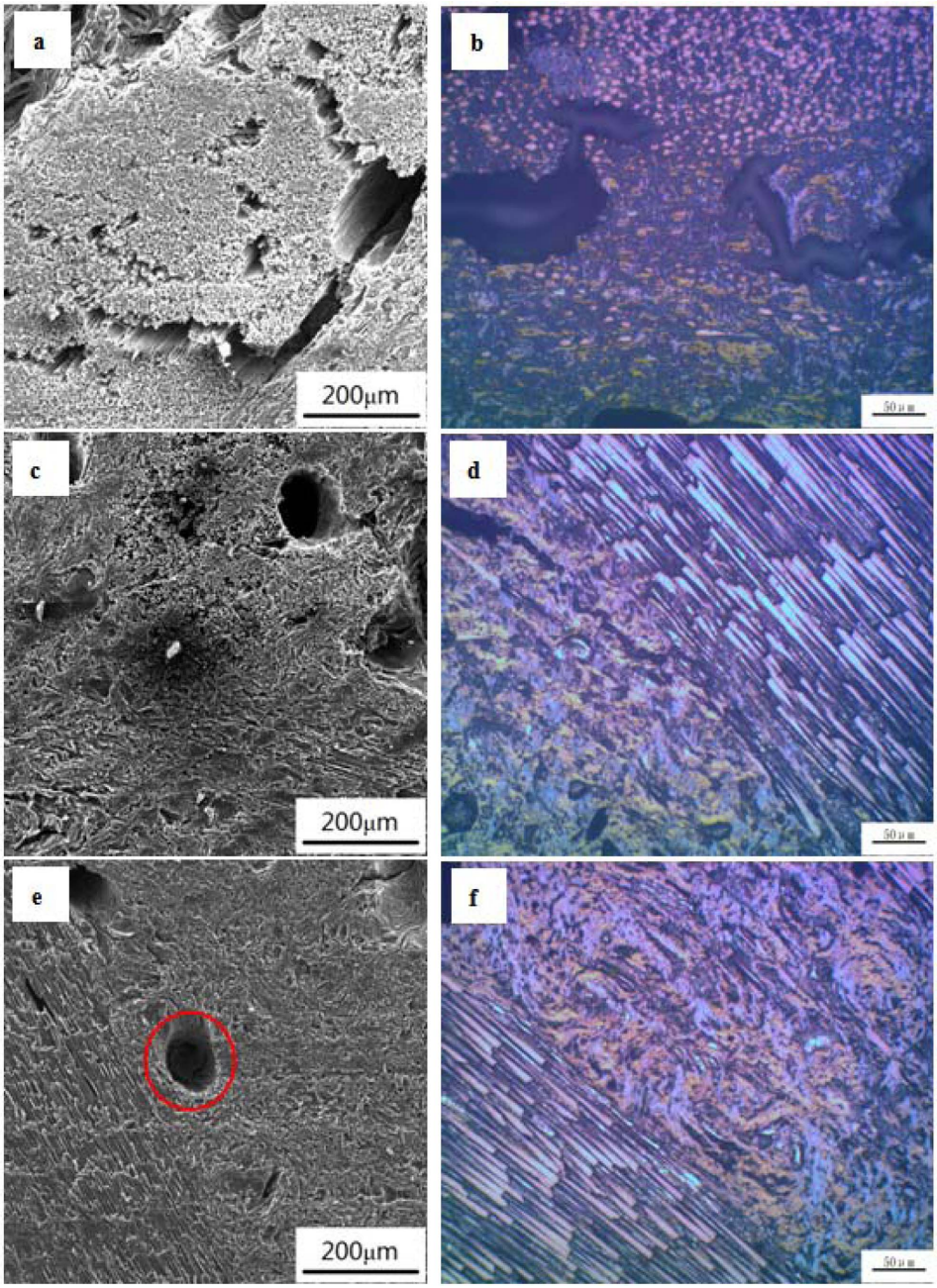

Fig. 1. SEM images and polarizing electronic microscope photos of C/C composites with different densities. (a, b) ρ=1.0 g·cm^{-3}, (c, d) ρ=1.4 g·cm^{-3}, (e, f) ρ=1.8 g·cm^{-3}.

20 μm (Fig. 2(b)) could be detected in the surface. By comparison, the composite with density of 1.8 g·cm^{-3} exhibited relatively denser microstructure with a few micro-cracks on its surface (Fig. 2(c)). There existed some large particles in local regions for the composite D1.8.

In order to get further insight into the internal microstructure of B_4C-SiC-ZrC-ZrB_2 coating for C/C composites subjected to heat treatment, the specimens were cut open along the longitudinal direction. Fig. 3 shows SEM images of cross section of the specimens with different densities. The interface profile between coating and matrix was clear and there was no porosity and crack, which could demonstrate the good combination. The phenomena are assumed to arise from gradient coating formation during the impregnation process. In addition, the polycarbosilane generated through pyrolysis reaction exhibited good physical compatibility with carbon materials. The interface stress was reduced during the heat treatment process. In Fig. 3(a), there existed some holes and cracks in the coating of B_4C-SiC-ZrC-ZrB_2 coating for C/C composites D1.0. The thickness of the coating was detected to be ca. 149-155 μm, turning thinner with elevating the density. The

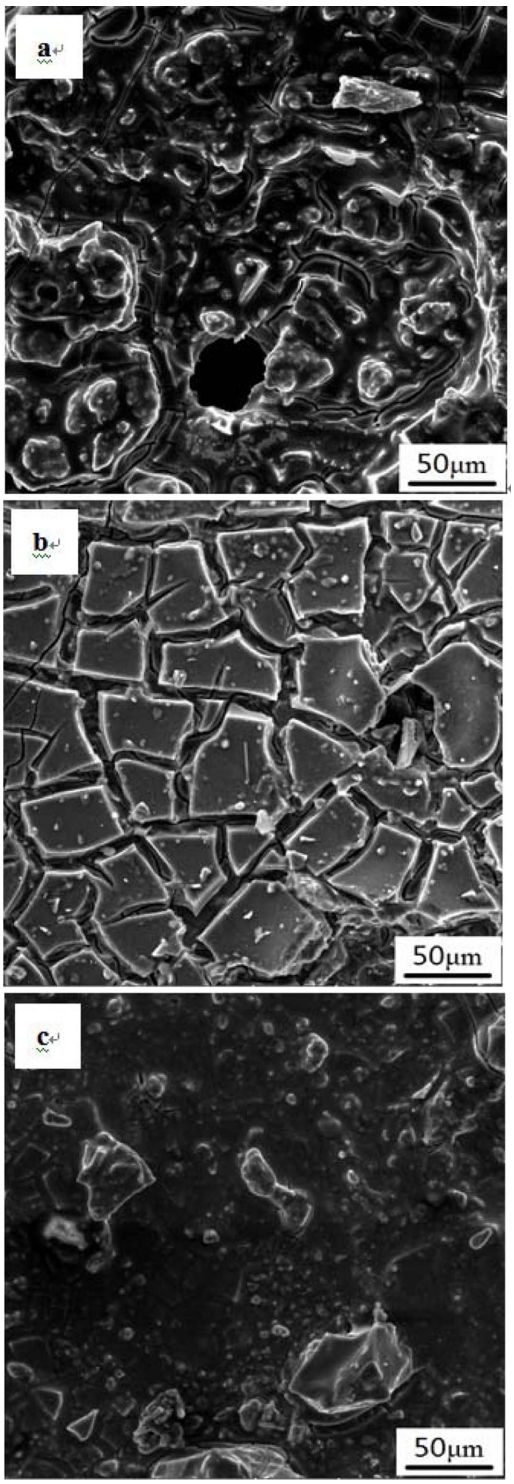

Fig. 2. SEM images of B_4C-SiC-ZrC-ZrB_2 coating for C/C composites after heat treatment at 1200 °C. (a) ρ=1.0 g·cm^{-3}, (b) ρ=1.4 g·cm^{-3}, (c) ρ=1.8 g·cm^{-3}.

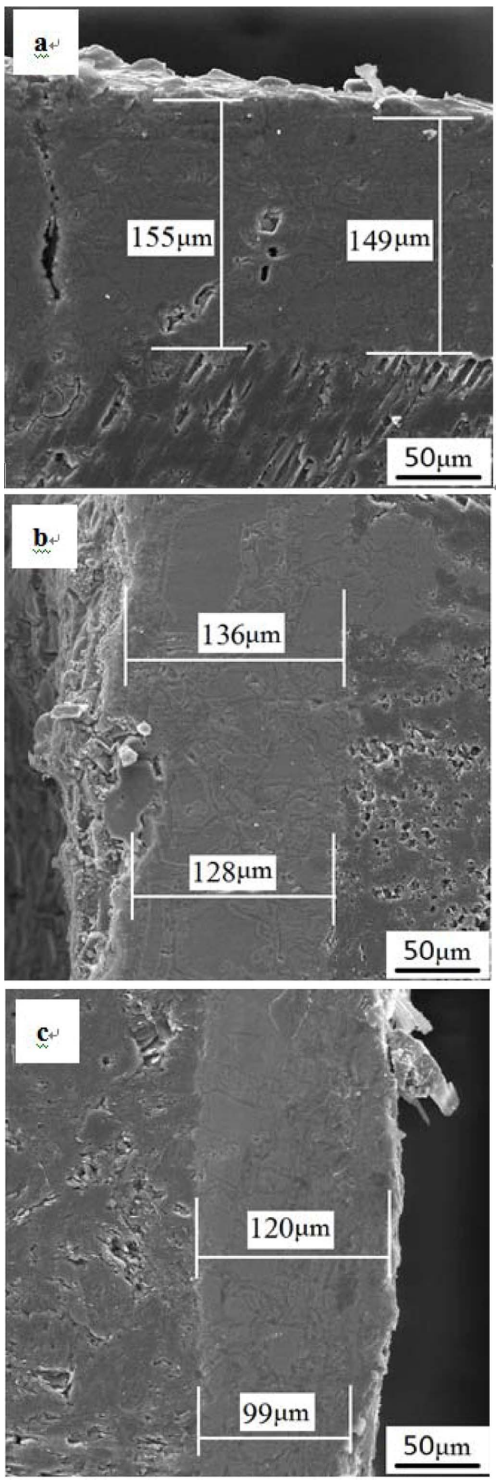

Fig. 3. SEM images of cross section view of C/C composites with B_4C-SiC-ZrC-ZrB_2 coating obtained by heat treatment at 1200 °C. (a) ρ=1.0 g·cm^{-3}, (b) ρ=1.4 g·cm^{-3}, (c) ρ=1.8 g·cm^{-3}.

surface coating thickness of the composites D1.4 and D1.8 were determined to be 128-136 μm and 99-120 μm, respectively (Fig. 3(b), 3(c)). The thickness of the coating may be related to the size and number of porosity and crack. The porosity and crack are well situated to benefit for the coating. The coating was found to grow denser as the density increased for the composite specimens. The composite D1.0 was examined to be more infiltration in quantity, resulting in much more small molecules escaping. By comparison, B_4C-SiC-ZrC-ZrB_2 coating for C/C composites D1.8 produced less volatile substance during pyrolysis process, leading

to denser microstructure and closer combination between the coating and matrix.

To look further into the oxidation resistance, we surveyed the evolution of weight loss on oxidation temperature for C/C composites with B_4C-SiC-ZrC-ZrB_2 coating. The composite samples were oxidized at 800-1,550 °C in air for 1 h. Fig. 4 shows the weight loss as a function of oxidation temperature for the specimens with different densities. For all composite specimens, the weight losses displayed monotonous increment with elevating oxidation temperature. At given oxidation temperature, the composite D1.0 revealed a larger weigh loss compared to the other specimens. The weight losses for the specimen D1.0 were determined to be 1.1 wt.% and 3.3 wt.% at the oxidation temperature of 800 °C and 1,550 °C, respectively. While the weight losses for the specimen D1.8 were detected to be 0.4 wt.% and 1.8 wt.%, respectively. It indicates that the weight loss rate is related to the oxidation temperature and the material density. One can notice that weight loss exhibited analogous variation with oxidation temperature for the composites D1.4 and D1.8. There existed three different stages, relatively flat at 800-1,000 °C, sharply incremental at 1,000-1,400 °C and basically invariable at 1,400-1,550 °C. In addition, there was almost no discrepancy in weight loss among the two composites. In the oxidation process, the oxidation for carbide and boride are favorable to the increment in the mass of composites. On the other hand, B_2O_3 and SiO_2 volatile, as well as carbon oxidation, will result in an opposite effect on the mass of composites. The evolution of weight loss appears to be dependent on the twofold effect. So the weight loss is dominated by the oxidation temperature and composition and structure of the composites.

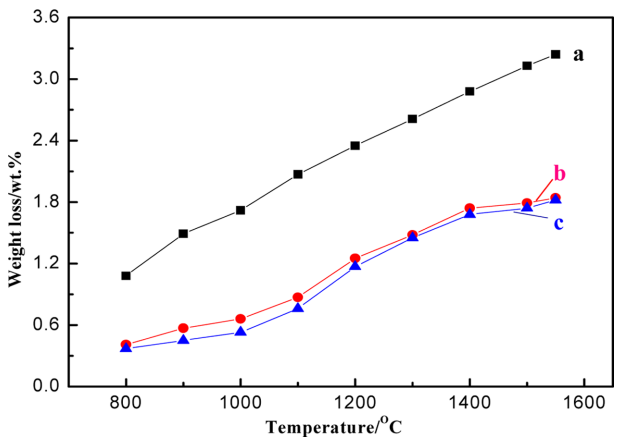

Fig. 4. Weight loss as a function of oxidation temperature for C/C composites with B_4C-SiC-ZrC-ZrB_2 coating with the density of (a) ρ=1.0 g·cm^{-3}, (b) ρ=1.4 g·cm^{-3}, (c) ρ=1.8 g·cm^{-3} in air for 1 h.

Fig. 5 shows XRD patterns of C/C composites with B_4C-SiC-ZrC-ZrB_2 coating with different densities and oxidation temperatures. D1.0, D1.4 and D1.8 refer to the composite sample with the density of 1.0, 1.4 and 1.8 g·cm^{-3}, respectively. One can observe that the composites consist of carbon, SiC, SiO_2 and ZrO_2. Fig. 5(c) shows the reference patterns of carbon (rhombohedral structure, JCPDS card NO. 26-1079), SiC (Hexagonal structure, JCPDS card NO. 29-1131), SiO_2 (tetragonal structure, JCPDS card NO. 39-1425) and ZrO_2 (nonoclinic structure, JCPDS card NO. 37-1484). The crystal structures were detected to be basically invariable for every composite regardless of density at oxidation temperature of 800 °C. The results can be explained in terms of the formation of oxide glass films, preventing oxygen diffusion into the composites. Therefore, it makes sense that the weight loss of the composite becomes less after oxidation. However, one can notice that the diffraction peak of SiC grows weaker and the peak of SiO_2 stronger when oxidation temperature rise to 1,500 °C. The finding is believed to be reasonable because of SiO_2 generation, originated from the reaction of SiC with permeating oxygen. The part SiO_2 generation can form glassy phase film in high temperature which is assumed to favor improving oxidation resistance of the composites.

To look further into the effect of oxidation on the internal microstructure, we investigate SEM images of transverse view for C/C composites with B_4C-SiC-ZrC-ZrB_2 coating after oxidation at 800 °C for 1 h (as shown in Fig. 6). Tight combination between the coating

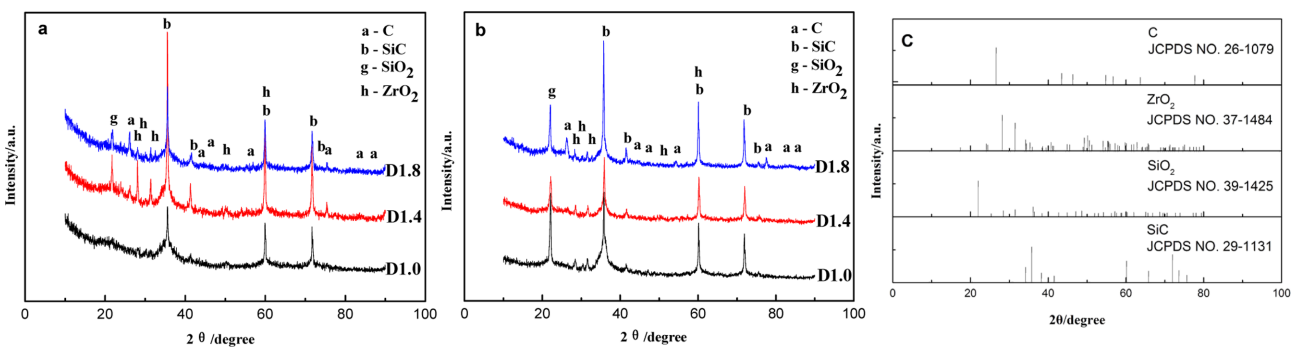

Fig. 5. XRD patterns of C/C composites with B_4C-SiC-ZrC-ZrB_2 coating with different densities and oxidation temperatures of (a) 800 °C and (b) 1,500 °C. (c) is the standard patterns of Carbon, ZrO_2, SiO_2 and SiC in the composites.

and carbon fibers was detected in the composite sample. The internal structure of carbon fiber remained a good integrity, indicating a good oxidation resistance for the composites at 800 ºC. The surface of the com−posite appears fairly rough owing to gas volatilization, such as B_2O_3, during the oxidation process.

Fig. 7 shows SEM images of transverse view for C/C composites with B_4C-SiC-ZrC-ZrB_2 coating with different densities after oxidation at 1,500 ºC for 1 h. As shown in Fig. 7(a), the composite D1.0 displayed loose surface structure and many holes existing in the interface between coating and substrate. These holes were due to matrix carbon combustion during oxidation at 1,500 ºC. The composite D1.4 showed apparent cracks through

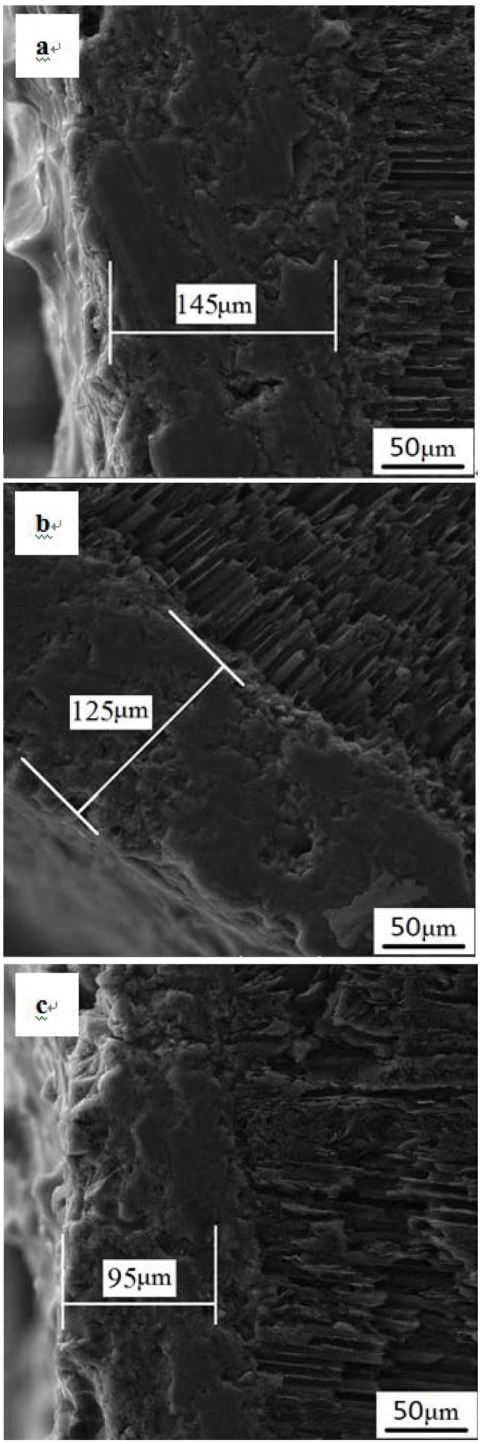

Fig. 6. SEM images of transverse view for C/C composites with B_4C-SiC-ZrC-ZrB_2 coating with the density of (a) ρ=1.0 g·cm^{-3}, (b) ρ=1.4 g·cm^{-3}, (c) ρ=1.8 g·cm^{-3} after oxidation at 800 ºC for 1 h.

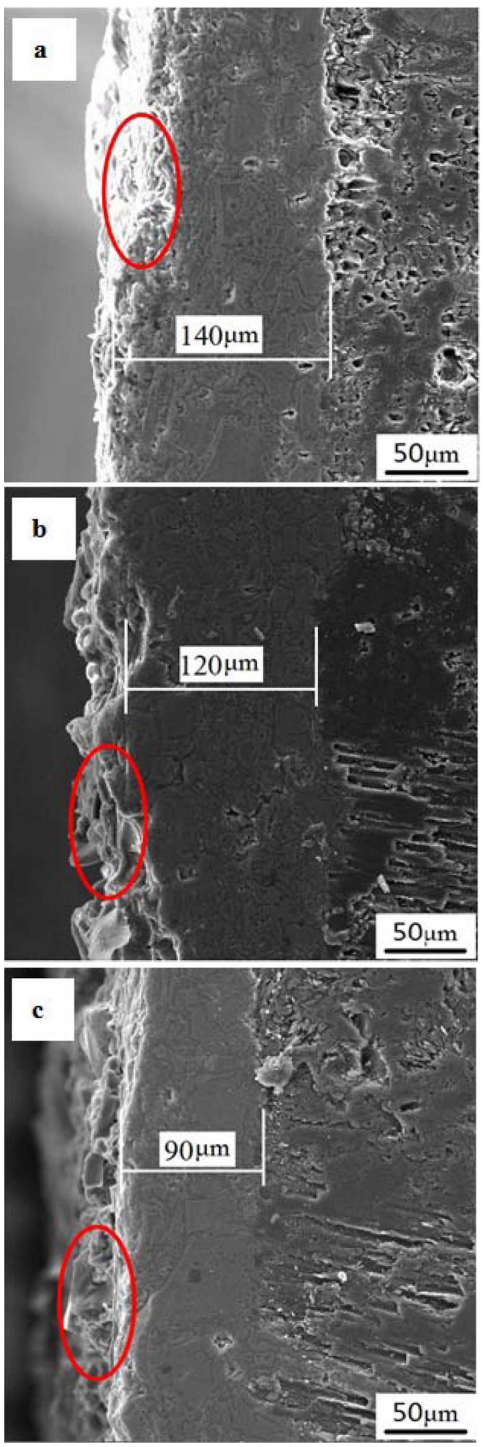

Fig. 7. SEM images of transverse view for C/C composites with B_4C-SiC-ZrC-ZrB_2 coating with the density of (a) ρ=1.0 g·cm^{-3}, (b) ρ=1.4 g·cm^{-3}, (c) ρ=1.8 g·cm^{-3} after oxidation at 1,500 ºC for 1 h.

the coating and intact interface structure between coating and matrix. The composite D1.8 exhibited a dense coating, effectively protecting the internal carbon fiber structure. One can observe that the coating become thinner after the oxidation at 1,500 ºC for all the composites. A violent reaction between the coating of the composites and ambient oxygen are believed to take place after oxidation of 1,500 ºC. The produced SiO_2 and B_2O_3 are volatile, resulting in the thickness reduction of the coating and crack appearing. On the other hand, ZrO_2 derived from the decomposition of zirconium-contained compound possesses a high melting point and good stability at high temperature. In addition, the oxide formed by the reaction of ZrO_2 and SiO_2 is beneficial to prevent the SiO_2 and B_2O_3 glass from consuming at high temperature.

Fig. 8 shows the SEM image and EDS analysis for C/C composites with B_4C-SiC-ZrC-ZrB_2 coating with a density of 1.8 g·cm^{-3} after oxidation at 1,500 ºC for 1 h. The mappings area was donoted in Fig. 8(a). EDS scanning was conducted from the coating to the inner layer, and finally through carbon materials in the matrix. As shown in Fig. 8b-8f, there existed more Si and oxygen element while less C and B elements in the coating of the composite. However, more C and B elements while less Si and oxygen elements were detected in the matrix of the composite. Zirconium element was found to be homogeneous distribution in the coating and matrix. Based on the EDS scanning results, B, Si and Zr elements were considered to penetrate into the surface of C/C composite. During the oxidation process at 1,500 ºC, B_4C-SiC-ZrC-ZrB_2 coating became thinner. Ambient oxygen diffused through the coating into the matrix of C/C composite. B, Si and Zr elements on the surface of the composite would form corresponding self-healing oxides, which could inhibit the further diffusion of oxygen and thus protect carbon matrix [18, 19].

Conclusions

In this study, B_4C-SiC-ZrC-ZrB_2 coating was designed and prepared for C/C composites by infiltration and pyrolysis. The phase compositions, surface morphologies and element distributions of the coating for the composites with the density of 1.0, 1.4 and 1.8 g·cm^{-3} were examined. The coating for the composites with the density of 1.4 g·cm^{-3} and 1.8 g·cm^{-3} exhibited compact microstructures and well-combination with the substrates. After exposure to air at 800-1,550 ºC for 1

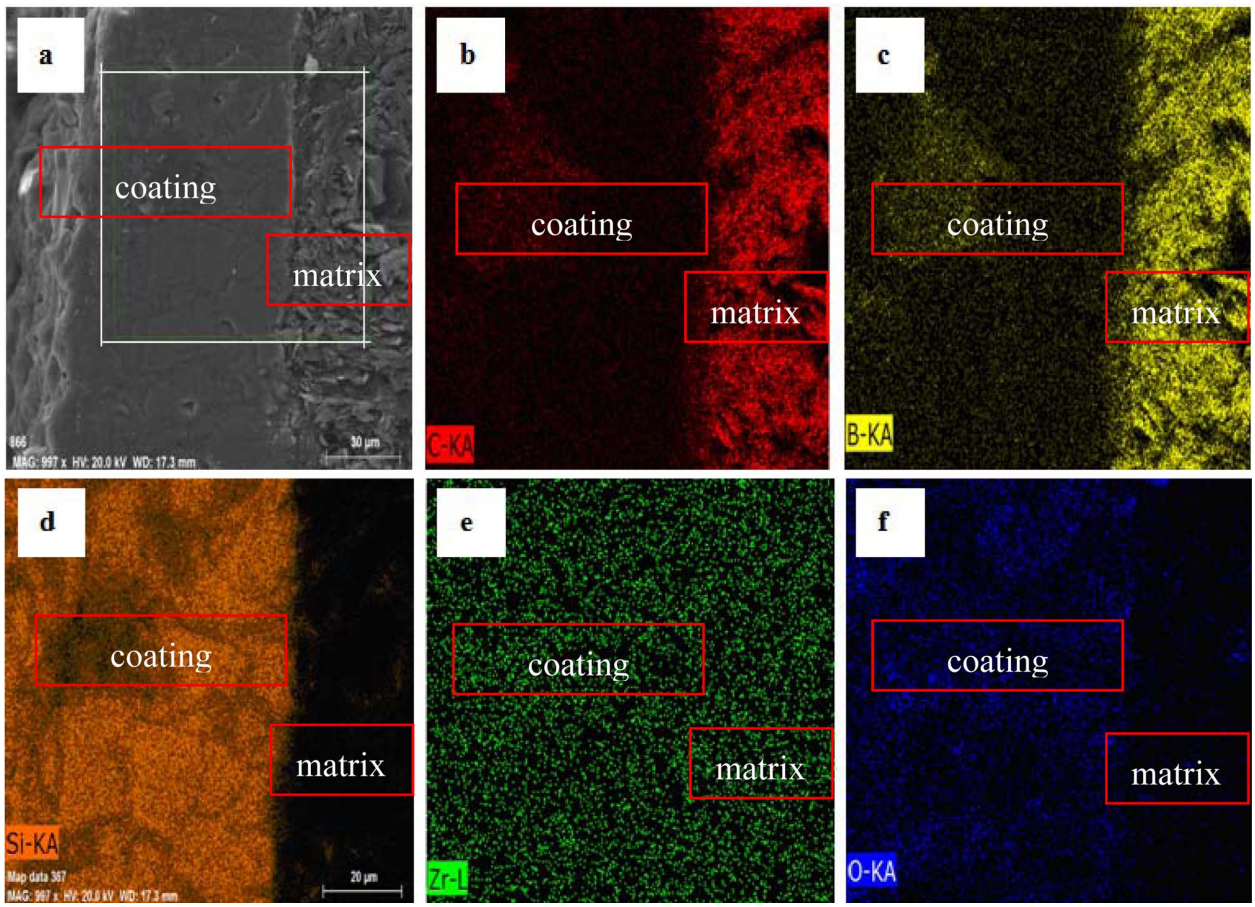

Fig. 8. SEM image of C/C composites with B_4C-SiC-ZrC-ZrB_2 coating after oxidation at 1,500ºC for 1h (a) D1.8 and its corresponding elemental mappings of (b) carbon, (c) boron, (d) silicon, (e) zirconium and (f) oxygen.

h, the weight loss of the composites was lower. The protective glassy films were deduced to be composed of B_2O_3, SiO_2 and ZrO_2, formed on the surface of the composites during the oxidation process. The coating for the composites with the density of 1.4 and 1.8 $g \cdot cm^{-3}$ can provide a good oxidation resistance at different temperature owing to the dense structure and self-healing oxide glass and synergistic effects. The oxide formed by the reaction of ZrO_2 and SiO_2 is beneficial to prevent the SiO_2 and B_2O_3 glass from consuming at high temperature in air. At the same time, the oxide glass can prevent oxygen from further diffusion into the matrix and thus improved the oxidation resistance of the composites.

Acknowledgements

This work was financially supported by National Natural Science Foundation of China (91016003, 51372077) and Scientific Research Fund of Hubei Polytechnic University and Huangshi city (13xjz02c, 2010A10193).

References

1. K.Z. Li, F.T. Lan, H.J. Li, X.T. Shen, and Y.G. He, J. Eur. Ceram. Soc. 29[9] (2009) 1803-1807.
2. S.Q. Guo, Y. Kwgawa, T. Nishimura, D. Chung, and J.M. Yang, J. Eur. Ceram. Soc. 28[6] (2008) 1279-1285.
3. Y.L. Zhang, H.J. Li, X.Y. Yao, K.Z. Li, and S.Y. Zhang, Surf. Coat. Technol. 206[2-3] (2011) 492-496.
4. X.T. Yang, H.F. Quan, and K. Wang. J. Alloys Compd. 836 (2020) 155532-155541.
5. B.S. Xu, R.J. He, C.Q. Hong, Y.B. Ma, W.B. Wen, H.M. Li, T.B. Cheng, D.N. Fang, and Y.Z. Yang, J. Alloys Compd. 702 (2017) 551-560.
6. Y.S. Liu, L.T. Zhong, L.F. Cheng, X.L.W. Yang. W.H. Zhang, Y. D. Xu, and Q. F. Zeng, Mater. Sci. Eng. A 498[1-2] (2008) 430-436.
7. A.V.K. Westwood, B. Rand, and S. Lu, Carbon. 42[15] (2004) 3071-3080.
8. Y.H. Seong, S.J. Lee, and D.K. Kim, J. Am. Ceram. Soc. 96[5] (2013) 1570-1576.
9. C.X. Liu, L.X. Cao, J.X. Chen, L. Xue, X. Tang, and Q.Z. Huang, Carbon. 65 (2013) 196-205.
10. X. Yang, Z.A. Su, Q.Z. Huang, X. Chang, C.Q. Fang, L. Chen, and G. Zeng, Ceram. Int. 42[16] (2016) 19195-19205.
11. A. Paul, S. Venugopal, J.G.P. Binner, B. Vaidhyanathan, A.C.J. Heaton, and P.M. Brown, J. Eur. Ceram. Soc. 33[2] (2013) 423-432.
12. Y.X. Chen, P. Chen, C.Q. Hong, B.X. Zhang, and D. Hui, Composites Part B: Engineering. 47 (2013) 320-325.
13. T. Tian, W. Sun, X. Xiong, Y.L. Xu, Y.T. Chen, Y. Zeng, and F.Q. Liu. J. Eur. Ceram. 39[4] (2019) 1696-1702.
14. D.N. Wang, Y. Zeng, X. Xiong, G.D. Li, Z.K. Chen, W. Sun, and Y.L. Wang, Ceram. Int. 41[6] (2015) 7677-7686.
15. C. Hu, Y.R. Niu, S.S. Huang, H. Li, M.S. Ren, Y. Zeng, X.B. Zheng, and J.L. Sun, J. Alloys Compd. 646 (2015) 916-923.
16. P. Wang, S.B. Zhou, X.H. Zhang, K.X. Gui, Y.X. Li, J.D. An, and W.B. Han, Surf. Coat. Technol. 280 (2015) 330-337.
17. X. Qing, W. Sun, T. Tian, X. Xiong, H.B. Zhang, Z.K. Chen, and Y. Zeng. Ceram. Int. 46[11] (2020) 18895-18902.
18. R.V. Krishnarao, Md. Zafir Alam, and D.K. Das, Corros. Sci. 141 (2018) 72-80.
19. R.V. Krishnarao, Z. Alam, D.K. Das, V.V.B. Prasad, and G.M. Reddy, Int. J. Refract. Met. Hard Mater. 52 (2015) 55-65.